Numerical study of the gluon propagator and confinement scenario in the minimal Coulomb gauge

Attilio Cucchieri*

IFSC-USP, Caixa Postal 369, 13560-970 São Carlos, SP, Brazil

Daniel Zwanziger†

Physics Department, New York University, New York, New York 10003

We present numerical results in $SU(2)$ lattice gauge theory for the space-space and time-time components of the gluon propagator at equal time in the minimal Coulomb gauge. It is found that the equal-time would-be physical 3-dimensionally transverse gluon propagator $D^{\text{tr}}(\vec{k})$ vanishes at $\vec{k}=0$ when extrapolated to infinite lattice volume, whereas the instantaneous color-Coulomb potential $D_{44}(\vec{k})$ is strongly enhanced at $\vec{k}=0$. This has a natural interpretation in a confinement scenario in which the would-be physical gluons leave the physical spectrum while the long-range Coulomb force confines color. Gribov's formula $D^{\text{tr}}(\vec{k})=(|\vec{k}|/2)[(\vec{k}^2)^2 + M^4]^{1/2}$ provides an excellent fit to our data for the 3-dimensionally transverse equal-time gluon propagator $D^{\text{tr}}(\vec{k})$ for relevant values of $\vec{k}$.

I. INTRODUCTION

Wilson's lattice gauge theory provides a regularized formulation of gauge theory that is manifestly gauge invariant, and numerical simulations do not require gauge fixing. However gauge fixing on the lattice is advantageous to gain control of the critical or continuum limit, for this makes available the strong results of gauge-fixed continuum renormalization theory. For example one may prove in continuum renormalization theory that a certain quantity, such as the running coupling constant, defined in terms of gluon correlation functions in some gauge, is finite when the cutoff is removed. Then the corresponding lattice quantity, defined in the corresponding lattice gauge, should be finite in the critical limit, and it becomes of interest to make a numerical determination of that quantity. Moreover one may determine by numerical fit the location of the poles of propagators which, according to the Nielsen identities, is independent of the gauge parameters [1]. Finally, if one has in hand a confinement scenario in a particular gauge, then it is possible to test its predictions numerically for gauge-fixed quantities. Although the scenario may look quite different in different gauges, nevertheless any one of them provides a valid perspective.

Previous numerical studies of the Coulomb gauge were reported in [2,3]. We present here a numerical study of the gluon propagator in $SU(2)$ lattice gauge theory, without quarks, in the minimal Coulomb gauge (defined in the Appendix). Simulations have been done at $\beta=2.2$ for 9 different lattice volumes $V=L^4$, with $L=14$, 16, 18, 20, 22, 24, 26, 28 and 30. (A total of 2420 configurations have been generated, from 50 configurations for 30^4 up to 600 for 14^4.) The procedure is to first equilibrate ungauge-fixed configurations U according to the Wilson action using a hybrid over-relaxed algorithm [4]. Then statistically independent configurations U are gauge fixed to the minimal lattice Coulomb gauge by a minimization that is effected using a stochastic over-relaxation algorithm described in [5] with accuracy $\langle(\partial_i A_i)^2\rangle \leq 10^{-16}$, where the average is taken on each time slice separately and $\partial_i A_i$ is defined in Eq. (A5). Finally the components $D^{\text{tr}}(\vec{k})$ and $D_{44}(\vec{k})$ of the *equal-time* gluon correlator are evaluated. The lattice Coulomb gauge is more easily accessible to numerical study than the Landau gauge because each time slice contributes separately to the numerical average which, for a lattice of volume 30^4, gives a factor of 30 gain. The total computer time devoted to this project so far is about 500 days on a 500 MHz ALPHA workstation.[1]

The results provide a test of the confinement scenario that was originally proposed by Gribov [6] and elaborated in [7]. The confinement scenario is particularly transparent in the Coulomb gauge because it is a physical gauge in the sense that the constraints are solved exactly, including Gauss's law $D_i E_i \equiv \partial_i E_i + [A_i, E_i] = \rho_{\text{qu}}$, and the Hilbert space has positive metric. Here E_i is the color-electric field, D_i is the gauge-covariant derivative, and ρ_{qu} is the color-charge density of quarks. Moreover the gauge fixing, described in the Appendix, is done independently within each time-slice so that the equal-time Euclidean and Minkowskian of the correlation functions are identical.

In the Coulomb gauge, the 3-vector potential A_i is transverse, $\partial_i A_i = 0$, so $A_i = A_i^{\text{tr}}$. Gauss's law is solved by

$$E_i = E_i^{\text{tr}} - \partial_i \phi, \tag{1}$$

where the color-Coulomb field ϕ is given by

$$\phi = M^{-1} \rho_{\text{coul}}. \tag{2}$$

---

*Electronic address: attilio@if.sc.usp.br

†Electronic address: daniel.zwanziger@nyu.edu

Here $\rho_{\text{coul}} \equiv \rho_{\text{qu}} - [A_i^{\text{tr}}, E_i^{\text{tr}}]$ is the color-charge density of the dynamical degrees of freedom, and $M = M(A^{\text{tr}}) = -D_i(A^{\text{tr}})\partial_i$ is the 3-dimensional Faddeev-Popov operator.

In this gauge, the Hamiltonian (without quarks) is given by

$$H = (2g_0^2)^{-1} \int d^3x (E^2 + B^2) \tag{3}$$

$$= (2g_0^2)^{-1} \int d^3x (E^{\text{tr}2} + B^2)$$

$$+ (2g_0^2)^{-1} \int d^3x d^3y \rho_{\text{coul}}(x) \mathcal{V}(x,y;A^{\text{tr}}) \rho_{\text{coul}}(y). \tag{4}$$

Here

$$\mathcal{V}(x,y;A^{\text{tr}}) \equiv [M(A^{\text{tr}})^{-1}(-\partial^2) M(A^{\text{tr}})^{-1}]_{x,y}^{\to\to} \tag{5}$$

is a color-Coulomb potential-energy functional, depending on A^{tr}, that acts instantaneously and couples universally to color charge. The continuum form of the Coulomb Hamiltonian, with proper attention to operator ordering is given in [8] and the lattice form in [9]. For the *minimal* Coulomb gauge, this Hamiltonian is supplemented by the boundary condition that the wave functionals $\Psi(A^{\text{tr}})$ are restricted to the Gribov region. (This is explained below and in the Appendix.) It was proposed in continuum theory in [6] and in lattice theory in [10], that this restriction may be imposed by use of an effective action or Hamiltonian

$$H_{\text{eff}} = H + (2g_0^2)^{-1} \int d^3x M^4 A_i^{\text{tr}}(-\nabla^2)^{-1} A_i^{\text{tr}}. \tag{6}$$

As a result, the energy of a gluon of momentum $\vec{k}$ gets modified to $E^2(\vec{k}) = \vec{k}^2 + (\vec{k}^2)^{-1} M^4$, as one sees from the quadratic part of H_{eff}. One obtains for the equal-time 3-dimensionally transverse would-be physical gluon propagator the approximate expression

$$D^{\text{tr}}(\vec{k}) = (2\pi)^{-1} \int dk_4 \frac{1}{k_4^2 + E^2(\vec{k})} = \frac{1}{2E(\vec{k})} \tag{7}$$

$$= \frac{|\vec{k}|}{2[(\vec{k}^2)^2 + M^4]^{1/2}}. \tag{8}$$

This quantity is defined by

$$D_{ij}^{\text{tr}}(\vec{k}) = (\delta_{ij} - \hat{k}_i\hat{k}_j) D^{\text{tr}}(\vec{k}), \tag{9}$$

where $D_{ij}^{\text{tr}}(\vec{k})$ is the Fourier transform of

$$D_{ij}^{\text{tr}}(\vec{x} - \vec{y}) = \langle A_i^{\text{tr}}(\vec{x},t) A_j^{\text{tr}}(\vec{y},t) \rangle. \tag{10}$$

In the absence of an estimate of corrections, one does not know how accurate Eq. (8) may be. However it was proven [11] that the lattice gluon propagator $D^{\text{tr}}(\vec{k})$ at infinite spatial lattice volume L^3 must indeed *vanish* at $\vec{k} = 0$,

$$\lim_{\vec{k} \to 0} D^{\text{tr}}(\vec{k}) = 0, \tag{11}$$

although the rate of approach of $D^{\text{tr}}(0,L)$ to 0, as a function of L, was not established, nor was it determined whether the renormalized gluon propagator also shares this property. The accuracy of Eq. (8), and the crucial question of the extrapolation to large L of $D^{\text{tr}}(\vec{k},L)$ are addressed in the numerical study reported here.

We have also evaluated the 4-4 component of the gluon propagator

$$D_{44}(\vec{x},t) \equiv \langle A_4(\vec{x},t) A_4(0,0) \rangle \tag{12}$$

at equal-time. In the minimal Coulomb gauge $D_{44}(\vec{x},t)$ is given by [12]

$$D_{44}(\vec{x},t) = V(\vec{x}) \delta(t) + P(\vec{x},t), \tag{13}$$

where $t = x_4$ is the Euclidean "time" and $P(\vec{x},t)$ is a non-instantaneous vacuum-polarization term. This gives

$$\int_{-\epsilon}^{+\epsilon} dt D_{44}(\vec{x},t) = V(\vec{x}) + o(\epsilon), \tag{14}$$

where $o(\epsilon)$ vanishes with ϵ. We call $V(\vec{x})$ the color-Coulomb potential. In momentum space Eq. (13) reads

$$D_{44}(\vec{k},k_4) = V(\vec{k}) + P(\vec{k},k_4), \tag{15}$$

where $\lim_{k_4 \to \infty} P(\vec{k},k_4) = 0$. In dimension $d < 4$, $V(\vec{x})$ coincides with

$$V_0(\vec{x} - \vec{y}) \equiv \langle \mathcal{V}(x,y;A^{\text{tr}}) \rangle. \tag{16}$$

However in $d = 4$ dimensions there is a mixing of $V(\vec{k})$ and $P(\vec{k},k_4)$ associated with divergences, and $V(\vec{k})$ differs from $V_0(\vec{k})$ by terms of the form $c_n g_0^{2n}/\vec{k}^2$ in each order of perturbation theory, as explained in detail in [12].

Stated simply, the confinement of color is caused by the predominantly long range of the color-Coulomb potential $V(\vec{x})$, corresponding to an enhancement of $V(\vec{k})$ at low $|\vec{k}|$. Note however that $V(\vec{x})$ is *not* the gauge-invariant energy eigenvalue of the quantum state of infinitely massive separated quarks. Nevertheless it is an important quantity. It may be used as an order parameter for color confinement [7], and it is the starting point for calculations of the ground-state wave-functional [13–15].

The rather surprising and counter-intuitive vanishing of $D^{\text{tr}}(\vec{k})$ at $\vec{k} = 0$, and the enhancement of $V(\vec{k})$ at $\vec{k} = 0$ in the minimal Coulomb gauge are both caused by the Gribov horizon. This is a boundary in the space of configurations $A_i^{\text{tr}}(\vec{x})$ defined by the condition that the Faddeev-Popov operator be positive, $M(A^{\text{tr}}) \geq 0$. The Gribov horizon represents the points where the lowest eigenvalue $\lambda_0(A^{\text{tr}})$ of $M(A^{\text{tr}})$ first goes negative. As shown in the Appendix, all configurations that contribute to the Euclidean functional integral in

the minimal Coulomb gauge are constrained to lie within the Gribov horizon. Because of entropy considerations (see Refs. [6,10]), the Euclidean probability gets concentrated near the horizon where the color-Coulomb interaction energy $\mathcal{V}(A^{\text{tr}})$, Eq. (5), diverges. This causes an enhancement of the instantaneous color-Coulomb potential $V(\vec{x})$. At the same time it places very severe bounds on the magnitude of the low momentum components of the gluon field.[2]

The Coulomb gauge does not offer any particular advantage for perturbative calculations and renormalization. However it is the finite limit of renormalizable gauges [19]. A valuable feature of this gauge is that the time-time component of the gluon propagator $D_{44}(\vec{k},k_4)$ is independent of both the cut-off Λ and the renormalization mass μ [7]. This holds separately for its instantaneous part $V(\vec{k})$. Thus the minimal Coulomb gauge allows us to introduce a running coupling constant by $g_{\text{coul}}^2(|\vec{k}|)=\text{const}\,\vec{k}^2V(\vec{k})$. The proportionality constant is determined by the condition that in the large-momentum or weak-coupling regime $g_{\text{coul}}^2(|\vec{k}|)$ satisfy the standard renormalization-group equation,

$$|\vec{k}|\frac{\partial g_{\text{coul}}}{\partial|\vec{k}|}=\beta_{\text{coul}}(g_{\text{coul}})=-(b_0 g_{\text{coul}}^3+b_1 g_{\text{coul}}^5+\dots)\tag{17}$$

where, for $SU(N)$ gauge theory without quarks, $b_0=(4\pi)^{-2}11N/3$, $b_1=(4\pi)^{-4}34N^2/3$. The proportionality constant is calculated in [12], with the result that for $SU(N)$ gauge theory without quarks

$$\vec{k}^2V(\vec{k})=\frac{12}{11}g_{\text{coul}}^2(|\vec{k}|/\Lambda_{\text{coul}}),\tag{18}$$

and more generally, with N_f quark flavors

$$\vec{k}^2V(\vec{k})=\frac{12N}{11N-2N_f}g_{\text{coul}}^2(|\vec{k}|/\Lambda_{\text{coul}}).\tag{19}$$

Here $\Lambda_{\text{coul}}\propto\Lambda_{\text{QCD}}$ is a finite QCD mass scale, characteristic of the Coulomb gauge, such that asymptotically in the weak-coupling regime

$$\vec{k}^2=\Lambda_{\text{coul}}^2\exp[(b_0 g_{\text{coul}}^2)^{-1}](b_0 g_{\text{coul}}^2)^r,\tag{20}$$

where $r\equiv b_1/b_0^2$. The ratio $\Lambda_{\text{coul}}/\Lambda_{\text{QCD}}$ may be obtained from a 2-loop calculation [12]. We conclude that in the minimal Coulomb gauge the running coupling constant of QCD may be obtained from a numerical determination of the equal-time 2-point function D_{44}, whereas in other gauges it must be obtained from a 3-point function. The running coupling constant g_{coul} that we have introduced is the QCD ana-

---

[2]A similar confinement scenario for the Landau gauge was proposed in [16,17]. It has also been verified numerically in the Landau gauge that typical (thermalized and gauge-fixed) configurations lie very close to the Gribov horizon [18].
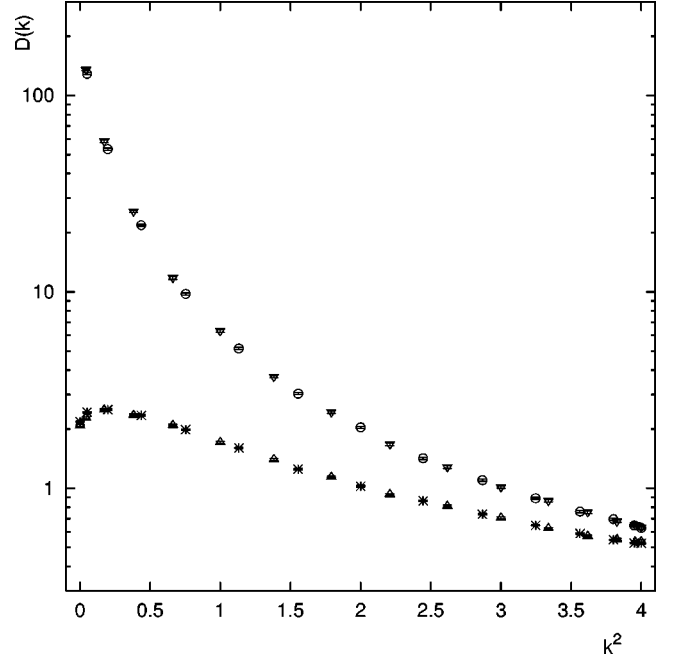

FIG. 1. Plot of the gluon propagators $D^{\text{tr}}(\vec{k})$ and $D_{44}(\vec{k})$ as a function of the square of the lattice momentum $\vec{k}^2$ for $L=28$ (symbols $*$ and $\bigcirc$ respectively) and $L=30$ (symbols $\triangle$ and $\bigtriangledown$ respectively). Notice the logarithmic scale in the y axis. Error bars are one standard deviation.

log of the invariant charge in QED that is defined in terms of the transverse part of the photon propagator in a Lorentz-covariant gauge.

II. RESULTS

We evaluate the space-space gluon propagator

$$D^{\text{tr}}(\vec{0})=\frac{1}{9V}\sum_{t=1}^{L}\sum_{\mu=1}^{3}\sum_{b=1}^{3}D_{\mu\mu}^{bb}(\vec{0},t)\tag{21}$$

$$D^{\text{tr}}(\vec{k})=\frac{1}{6V}\sum_{t=1}^{L}\sum_{\mu=1}^{3}\sum_{b=1}^{3}D_{\mu\mu}^{bb}(\vec{k},t),\tag{22}$$

and the time-time gluon propagator

$$D_{44}(\vec{k})=\frac{1}{3V}\sum_{t=1}^{L}\sum_{b=1}^{3}D_{44}^{bb}(\vec{k},t),\tag{23}$$

where

$$D_{\mu\mu}^{bb}(\vec{k},t)=\left\langle\left\{\left[\sum_{\vec{x}}A_{\vec{x}t\mu}^b\cos(\vec{\theta}\cdot\vec{x})\right]^2+\left[\sum_{\vec{x}}A_{\vec{x}t\mu}^b\sin(\vec{\theta}\cdot\vec{x})\right]^2\right.\right.\tag{24}$$

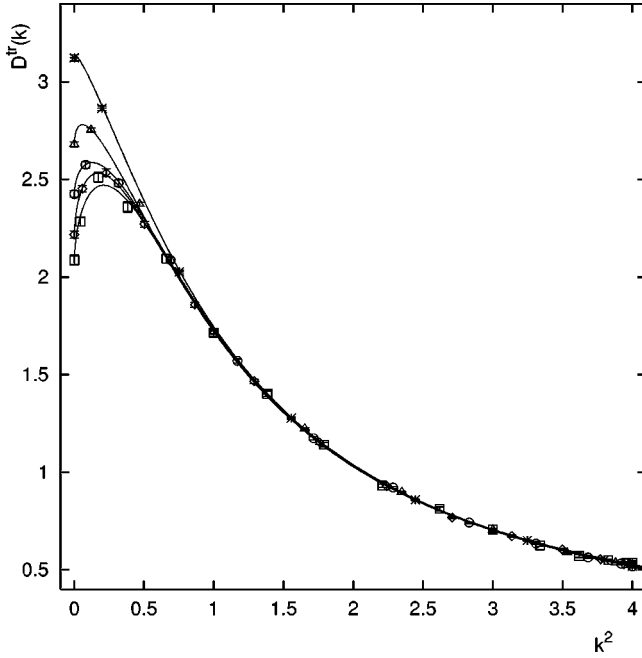and the lattice gluon field $A_{\vec{x}t\mu}^b$ is defined in Eq. (A6). Here,

FIG. 2. Plot of the gluon propagator $D^{\mathrm{tr}}(\vec{k})$ as a function of the square of the lattice momentum $\vec{k}^2$ for $L=14$ (*), 18 ($\triangle$), 22 ($\bigcirc$), 26 ($\diamond$), and 30 ($\square$) and fits of these data using Eq. (31) with the parameter values reported in Table I. Error bars are one standard deviation.
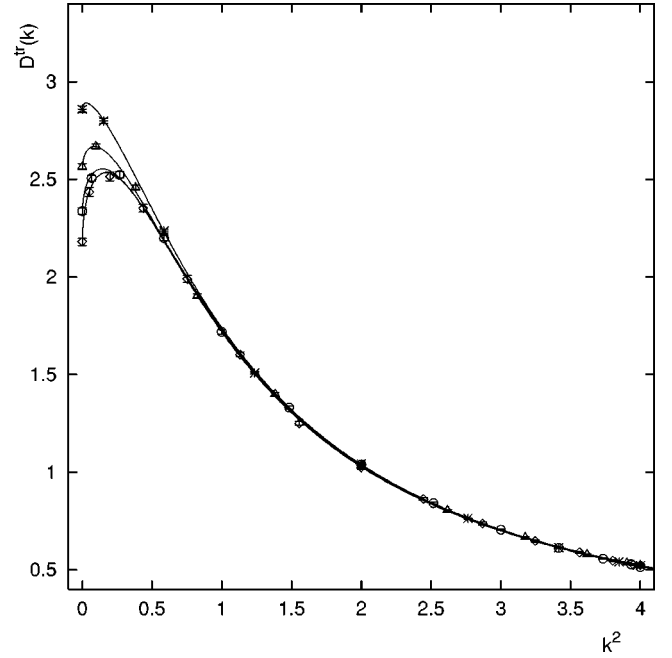
FIG. 3. Plot of the gluon propagator $D^{\mathrm{tr}}(\vec{k})$ as a function of the square of the lattice momentum $\vec{k}^2$ for $L = 16$ (*), 20 ($\triangle$), 24 ($\bigcirc$) and 28 ($\diamond$) and fits of these data using Eq. (31) with the parameter values reported in Table I. Error bars are one standard deviation.

as usual, we have defined $k_i \equiv 2 \sin(\theta_i/2)$, for $-\pi \leq \theta_i = 2\pi n_i/L \leq \pi$, and integer n_i. An average over the L time slices is included. In our simulations we consider only 3-momenta aligned along major axes $\theta_i = (0,0,2\pi n/L)$. Notice that $D^{\mathrm{tr}}(\vec{0})$ is not given by $D^{\mathrm{tr}}(\vec{k})$ at $\vec{k}=\vec{0}$. The difference is due to the Coulomb gauge condition — the continuum-like condition, Eq. (A5) — which in momentum space reads

$$\sum_{i=1}^{3} k_i \tilde{A}_{\vec{k}ti} = 0, \tag{25}$$

where $\tilde{A}_{\vec{k}ti}$ is the three-dimensional Fourier transform of the gauge field $A_{\vec{x}ti}$. If $\vec{k} \neq (0,0,0)$ only two of the three Lorentz components of $\tilde{A}_{\vec{k}ti}$ — and therefore of $A_{\vec{x}ti}$ — are independent. This explains the factor 6 (instead of 9) in the definition of $D^{\mathrm{tr}}(\vec{k})$.

Figure 1 shows $D^{\mathrm{tr}}(\vec{k})$ and $D_{44}(\vec{k})$ as a function of $\vec{k}^2$ on the same logarithmic plot for the lattice sides $L=28$ and 30. The qualitative behavior is quite different in the two cases. Whereas $D_{44}(\vec{k})$ grows strongly at low $\vec{k}$, by contrast $D^{\mathrm{tr}}(\vec{k})$ turns over and decreases at low $\vec{k}$.

(a) Analysis of D^{tr}. Figures 2 and 3 show our data for $D^{\mathrm{tr}}(\vec{k})$ for the nine lattice volumes considered. To param-

etrize these data, we were guided by the Nielsen identities [1]. They tell us that the poles of the gluon propagator $D^{\mathrm{tr}}(\vec{k},k_4)$ are independent of the gauge parameters.[3] In particular, for the class of gauges defined by $\lambda \partial_4 A_4 + \partial_i A_i = 0$, which interpolate between the Landau gauge, $\lambda = 1$, and the Coulomb gauge, $\lambda = 0$, the poles are independent of λ. In the Landau gauge, the poles occur at $k^2 = \vec{k}^2 + k_4^2 = -m^2$, by Lorentz (Euclidean) invariance, and thus also in all these gauges, by virtue of the Nielsen identities. We have made a 2-pole fit with poles at m_1^2 and m_2^2, which may be either a pair of real numbers or a complex conjugate pair.[4] According to [11], the propagator in the minimal Coulomb gauge vanishes at $\vec{k} = 0$. We use this condition to fix the residues to within an over-all normalization

---

[3] Strictly speaking, the Nielsen identities have been established only for Faddeev-Popov type gauge fixing. This does not include the minimal Coulomb gauge because the gauge fixing is done by a minimization procedure that is not describable by a local 4-dimensional action. However the minimal Coulomb gauge may be obtained as a limiting case of a local 5-dimensional quantum field theory that describes stochastic quantization with stochastic gauge fixing, as has been discussed recently in [16,17]. The Nielsen identities may be extended to the 5-dimensional formulation.

[4] According to the general principles of quantum field theory, the propagator of physical particles should have poles only at real positive m^2. However in the confined phase the gluon propagator may have singularities that correspond to unphysical excitations.

TABLE I. Fit of the transverse gluon propagator $D^{\mathrm{tr}}(\vec{k})$ using Eq. (31). The resulting fitting parameters, $\chi^2/\mathrm{d.o.f.}$ and goodness-of-fit Q are reported for each lattice side L.

L	z	r	α	x	y^2	$\chi^2/\mathrm{d.o.f.}$	Q
14	3.93(33)	3.86(35)	0.76(5)	0.36(6)	1.07(5)	0.42	73.9%
16	4.79(42)	2.72(28)	0.70(5)	0.27(8)	1.08(7)	1.46	21.1%
18	5.91(53)	2.27(33)	0.57(7)	0.38(13)	1.11(13)	3.45	0.4%
20	5.78(19)	1.80(8)	0.66(2)	0.19(4)	0.99(4)	0.45	84.5%
22	5.81(23)	1.57(8)	0.67(3)	0.09(4)	0.97(5)	0.59	76.5%
24	6.33(25)	1.43(8)	0.62(3)	0.12(4)	0.99(6)	0.86	55.0%
26	6.99(22)	1.08(5)	0.62(2)	0.12(3)	0.82(4)	0.60	79.8%
28	7.21(28)	1.05(6)	0.60(3)	0.14(4)	0.82(5)	0.72	70.6%
30	7.08(45)	0.93(8)	0.64(4)	0.06(6)	0.78(8)	1.54	11.0%

$$D^{\mathrm{tr}}(\vec{k},k_4)=C(\vec{k}^2)^{\alpha-1}\left(\frac{k_4^2+m_1^2}{\vec{k}^2+k_4^2+m_1^2}-\frac{k_4^2+m_2^2}{\vec{k}^2+k_4^2+m_2^2}\right) \quad (26)$$

$$=-C(\vec{k}^2)^{\alpha}\left(\frac{1}{\vec{k}^2+k_4^2+m_1^2}-\frac{1}{\vec{k}^2+k_4^2+m_2^2}\right), \quad (27)$$

where α is a fitting parameter. This formula does not reproduce the correct asymptotic behavior at large momenta $\sim(\vec{k}^2+k_4^2)^{-1}$ times logarithmic corrections. However, this is not a problem because our largest value of $|\vec{k}|$ is less than 2 GeV, and we are probably far from the ultraviolet regime.[5] We wish to emphasize that our pole parameters — to the extent that they are a valid fit — are gauge-independent quantities that characterize the gluon.

The equal-time part of this propagator is given by $D^{\mathrm{tr}}(\vec{k})=(2\pi)^{-1}\int d\theta_4 D^{\mathrm{tr}}(\vec{k},k_4)$, where $k_4=2\sin(\theta_4/2)$. This gives

$$D^{\mathrm{tr}}(\vec{k})=-C'(\vec{k}^2)^{\alpha}(A_1^{-1/2}-A_2^{-1/2}) \quad (28)$$

$$=C''(\vec{k}^2)^{\alpha}\frac{4+h_1+h_2}{A_1^{1/2}A_2^{1/2}(A_1^{1/2}+A_2^{1/2})}, \quad (29)$$

where $h_i\equiv vk^2+m_i^2$ and $A_i\equiv 4h_i+h_i^2$ for $i=1,2$. If we take a pair of complex conjugate poles, $m_1^2=x+iy$ and $m_2^2=x-iy$, we obtain

$$D^{\mathrm{tr}}(\vec{k})=C'''(\vec{k}^2)^{\alpha}\frac{v}{(u^2+4y^2v^2)^{1/2}[(u^2+4y^2v^2)^{1/2}+u]^{1/2}}, \quad (30)$$

where $u\equiv 4(\vec{k}^2+x)+(\vec{k}^2+x)^2-y^2$ and $v\equiv(2+\vec{k}^2+x)$. The case of a pair of real poles is obtained from this formula by taking a negative value of y^2. For the case of a lattice of finite volume $V=L^4$, we modify this formula to

$$D^{\mathrm{tr}}(\vec{k})=z[(\vec{k}^2)^{\alpha}+r]\frac{v}{(u^2+4y^2v^2)^{1/2}[(u^2+4y^2v^2)^{1/2}+u]^{1/2}}. \quad (31)$$

The factor

$$v[(u^2+4y^2v^2)^{1/2}+u]^{-1/2}$$
$$=(A_1-A_2)[8^{1/2}iy(A_1^{1/2}+A_2^{1/2})]^{-1}$$

is slowly varying over the relevant range of $\vec{k}$ and parameter values, so a fit to Eq. (31) is a test of the simpler formula

$$D^{\mathrm{tr}}(\vec{k})=z'[(\vec{k}^2)^{\alpha}+r]\frac{1}{(u^2+4y^2v^2)^{1/2}}. \quad (32)$$

Stated differently, Eqs. (31) and (32) have the same singularities that are nearest to the origin. In the continuum limit we have $u\rightarrow 4(\vec{k}^2+x)$ and $v\rightarrow 2$, and Eq. (32) is a lattice discretization of Gribov's approximate formula (8) provided that the fitting parameters have the values $r=0$, $\alpha=0.5$, $x=0$, with the identification $y^2=M^4$. It is intended to report on the fit to Eq. (32) elsewhere, but preliminary indications are that it is comparable in quality to the fit to Eq. (31).

For each lattice side L we have made a fit of the parameters $z(L),r(L),\alpha(L),x(L)$ and $y^2(L)$. By using Table 3 of [21] and by setting the physical string tension equal to $\sqrt{\sigma}=0.44$ GeV we obtain that, for $\beta=2.2$, the inverse lattice spacing is $a^{-1}=0.938$ GeV. This gives $a=0.21$ fm, so that the largest lattice volume considered here, i.e. $V=30^4$, corresponds to $(6.3\ \mathrm{fm})^4$, the smallest non-zero momentum that can be considered for that lattice is equal to 0.196 GeV, while the maximum momentum value (for each lattice side L) is 1.876 GeV. The results[6] are exhibited in Table I, and

---

[5] In the Landau gauge [20] the gluon propagator reaches three-loop asymptotic scaling at momenta of about 5–6 GeV.

[6] The fits have been done using gnuplot; the errors represent 68.3% confidence interval. Similar results have been obtained using a conjugate-gradient method with errors estimated by a jack-knife method. Let us notice that we did not consider the correlations between different momenta when fitting the data. However, at least in the Landau gauge, the covariance matrix for the gluon propagator in momentum space is essentially diagonal [22], and the value of the "naive" $\chi^2/\mathrm{d.o.f.}$ is usually compatible with the value obtained using the full covariance matrix [23].

TABLE II. Extrapolation to infinite lattice side L for the five fitting parameters appearing in Eq. (31) (we always have $r=0$). Five different cases are considered (see Sec. II).

$\vec{k}^2_{\min}$	No. data points	z	α	x	y^2	χ^2/d.o.f.	Q
		17.2(249)	0.48(5)	$-0.2(1)$	0.45(1)		
0.5	23	12.8(20)	0.45(7)	0.11(17)	0.45(6)	0.98	48.1%
0.3	25	13.4(11)	0.43(4)	0.17(8)	0.42(3)	0.94	53.8%
0.5	23	11.5(2)	0.49(1)	0	0.47(4)	0.96	50.9%
0.3	25	11.1(1)	0.51(1)	0	0.39(2)	1.22	21.7%

the curves are plotted in Figs. 2 and 3. There is no *a priori* reason why a 2-pole fit should be accurate over the whole range of momenta considered. However the fit is excellent for all momenta $\vec{k}^2$ and for each L. We have also checked that results in agreement with those reported in Table I are obtained if one considers only the data corresponding to $\vec{k}^2 < 2$.

We have extrapolated to infinite L the fitting parameters $z(L), \alpha(L), x(L), y^2(L)$ and the product $(rz)(L)$; in all cases we tried three different types of fitting functions, namely $a + b/L^c$, $\exp(a)/L^b$ and $a + \log(1+b/L)$, and we chose the fit with smallest χ^2/d.o.f. Results[7] are shown in Table II (first row) and plotted in Figs. 4–8.

The reader will have noticed that the product $(rz)(L)$ extrapolates to 0 (see Fig. 8). This corresponds to a *vanishing* of $D^{\text{tr}}(0)$ at infinite lattice volume, in accordance with [11]. To check on this important point we have also fitted $D^{\text{tr}}(0,L)$ using the three fitting functions considered above. A good fit is provided by $D^{\text{tr}}(0,L) = \exp(a)/L^b$, with $a = 2.43(4)$, $b = 0.50(1)$, χ^2/d.o.f. $= 0.69$ and goodness-of-fit $Q = 65.6\%$ (see Fig.9).[8] An indication of how reliable these fits are is the comparison of the power b in the fit of the product $(rz)(L)$ and of $D^{\text{tr}}(0,L)$ which are $b = 1.1(1)$ and $b = 0.50(1)$ respectively. We have also made a similar fit for $r(L)$ (not plotted) and obtained $b = 1.8(1)$.

We next consider the $\vec{k}$ dependence of $D^{\text{tr}}(\vec{k})$ at low $\vec{k}$. For the power dependence parametrized by $(\vec{k}^2)^\alpha$, observe that $\alpha(L)$ extrapolates to $\alpha(\infty) = 0.48(5)$, see Fig. 5. This agrees with Gribov's approximate formula (8), which gives $\alpha = 0.5$. Moreover this value is consistent with the other rows of Table II, by the method described below, so this result appears quite stable. Particularly striking is that, with $x = 0$ imposed, one obtains $\alpha = 0.49(1)$ and $\alpha = 0.51(1)$ respectively from the fourth and fifth rows of Table II (explained below).

Another striking feature of the fit is that $y^2(L)$ is positive for all 9 values of L (see Table I), corresponding to a pair of

complex conjugate poles rather than a pair of real poles. Moreover, in all cases $x(L)$ is quite small compared to $y(L)$. For example $x(30) = 0.06(6)$ and $y(30) = 0.88(5)$. The extrapolation to infinite L also strongly indicates a positive value $y^2(\infty) > 0$ and a small, possibly zero, value for $x(\infty)$. Thus our data are compatible with and perhaps suggestive of poles at purely imaginary $m^2 = 0 \pm iy$, in agreement with Gribov's formula (8) with $y^2 = M^4$.

Finally, we have fit the data for $L = 28$ and $L = 30$ using Eq. (31) with $r = 0$ and with a low-momentum cut $\vec{k}^2_{\min}$, namely considering only a range of momenta in which finite-size effects are negligible. Results are reported in the second and third rows of Table II for two different values of $\vec{k}^2_{\min}$. Similar results are also obtained when the fixed value $x = 0$ is imposed (see the last two rows of Table II and Fig. 10). The values for α and y^2 obtained in this way are in good agreement with the values obtained by extrapolating $\alpha(L)$ and $y^2(L)$ to infinite L (compare the first row of Table II with the other four rows of the same table).

(b) *Analysis of* D_{44}. Equation (14) shows that for lattice quantities we may make the identification $V(\vec{x}) = D_{44}(\vec{x})$, where $D_{44}(\vec{x})$ is the equal-time propagator, and similarly for their 3-momentum transforms, $V(\vec{k}) = D_{44}(\vec{k})$. This allows us to use Eqs. (23) and (18) to also define the lattice quantity $g^2_{\text{coul}}(\vec{k})$ by

$$\frac{12}{11} g^2_{\text{coul}}(\vec{k}) \equiv \vec{k}^2 V(\vec{k}) \equiv \vec{k}^2 D_{44}(\vec{k}). \qquad (33)$$

Figure 11 shows our data for the running coupling constant $\frac{12}{11} g^2_{\text{coul}}(\vec{k})$. In the continuum limit, its behavior at large momentum is governed by the perturbative renormalization group (17) and (20). For the fitting formula we modify Eq. (20) to

$$\vec{k}^2 = \Lambda^2_{\text{coul}} \exp[(b g^2_{\text{coul}})^{-1}][(b g^2_{\text{coul}})^{-r} + z(b g^2_{\text{coul}})^\alpha]^{-1}, \qquad (34)$$

which implicitly defines $g^2_{\text{coul}}(\vec{k}^2)$. Here $r = 102/121$, and $\Lambda^2_{\text{coul}}, b, z, \alpha$ are fitting parameters whose significance we now explain. Naturally the parameter Λ^2_{coul} sets the mass scale. For small g^2_{coul}, which corresponds to large $\vec{k}^2$, this formula is dominated by the first term in the denominator, whereas for large g^2_{coul}, which corresponds to small $\vec{k}^2$, it is

---

[7]These fits have also been done using GNUPLOT. For the fitting function $\exp(a)/L^b$ the results have been checked with the exact minimizing formula (notice that this fitting function is linear in the coefficients a and b after taking the logarithm).

[8]When using the fitting function $a + b/L^c$ we obtain, both for $(rz)(L)$ and $D^{\text{tr}}(0,L)$, a value of a that is zero within errors but a worse χ^2/d.o.f.
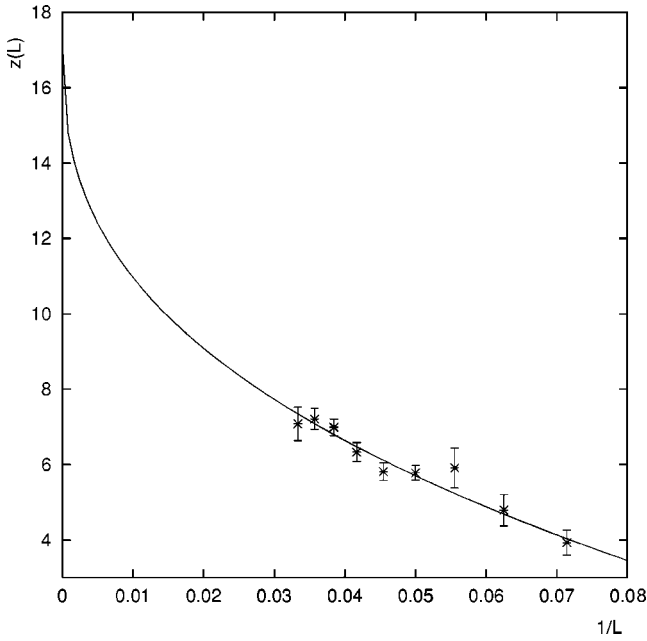
FIG. 4. Fit of the parameter $z(L)$ (see Table I) as a function of $1/L$ using $a - b/L^c$. We obtain $a = 17.2(249)$, $b = 35.9(117)$, $c = 0.38(83)$, $\chi^2/\text{d.o.f.} = 0.89$ and goodness-of-fit $Q = 50.1\%$.
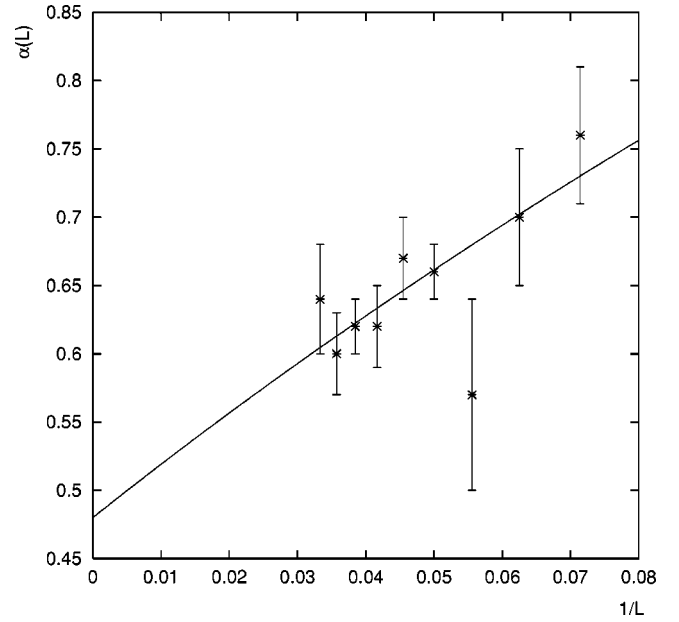

FIG. 5. Fit of the parameter $\alpha(L)$ (see Table I) as a function of $1/L$ using $a + \log(1 + b/L)$. We obtain $a = 0.48(5)$, $b = 4.0(13)$, $\chi^2/\text{d.o.f.} = 0.66$ and goodness-of-fit $Q = 70.6\%$.

dominated by the second term in the denominator. For small g_{coul}^2 the formula approaches Eq. (20), provided that $b = b_0 = 11/24\pi^2 \approx 0.046$. However we are quite far from the continuum limit for $D_{44}(\vec{k})$, as indicated by the small value $\langle (1/2)\text{tr}(U_4) \rangle = 0.221(6)$ (for lattice volume 14^4),[9] and we expect significant β-dependence in the extrapolation to the continuum limit. Moreover, for fixed β, it has been found that different lattice discretizations of the gluon field lead to identical gluon propagators to within numerical accuracy, apart from the overall normalization [24]. We allow for this by taking the overall normalization of g_{coul}^2 to be a fitting parameter. This requires putting an arbitrary normalization coefficient everywhere in front of g_{coul}^2 in Eq. (34), which is equivalent to replacing the fixed number b_0 by the fitting parameter b. Of course, an extrapolation in β to the continuum limit should give $b = b_0$.

For large g_{coul}^2 and small $\vec{k}^2$, this formula approaches

$$b g_{\text{coul}}^2 = \left(\frac{\Lambda_{\text{coul}}^2}{z\vec{k}^2} \right)^{1/\alpha}. \qquad (35)$$

Thus the parameter z sets the overall normalization in the strong-coupling or infrared regime, and α governs the strength of the singularity of g_{coul}^2 in the infrared limit. If the color-Coulomb potential $V(\vec{k})$ is governed by a string tension at large distances then $g_{\text{coul}}^2(\vec{k}) \sim \text{const}/\vec{k}^2$, which corresponds to $\alpha = 1$.

_____

[9]Before minimizing F_{ver} we find $\langle (1/2)\text{tr}(U_4) \rangle = -0.0005(57)$.

On a finite periodic lattice with finite lattice spacing and with $g_{\text{coul}}^2(\vec{k})$ defined by $\frac{12}{11} g_{\text{coul}}^2(\vec{k}) \equiv \vec{k}^2 V(\vec{k})$, necessarily $g_{\text{coul}}^2(\vec{k})$ vanishes at $\vec{k} = 0$. Actually $g_{\text{coul}}^2(\vec{k})$ gets a maximum value at $\vec{k}^2 \approx 0.2$ and goes to zero in the infrared limit (see Fig. 11). This unphysical behavior is a lattice artifact that also appears in studies of the running coupling constant using the three-gluon vertex [25]. In order to fit our data we have made a low-momentum cut at $\vec{k}_{\text{min}}^2 = 0.5$. The values of
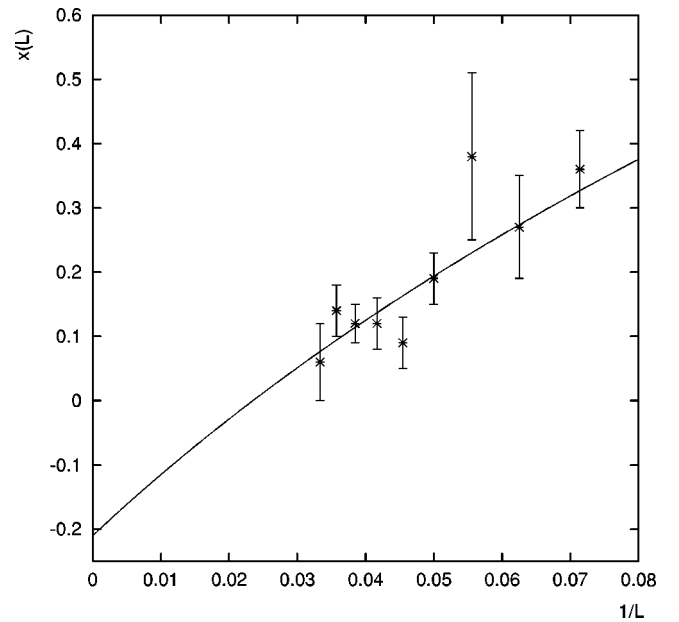

FIG. 6. Fit of the parameter $x(L)$ (see Table I) as a function of $1/L$ using $a + \log(1 + b/L)$. We obtain $a = -0.2(1)$, $b = 10.0(34)$, $\chi^2/\text{d.o.f.} = 0.94$ and goodness-of-fit $Q = 47.4\%$.
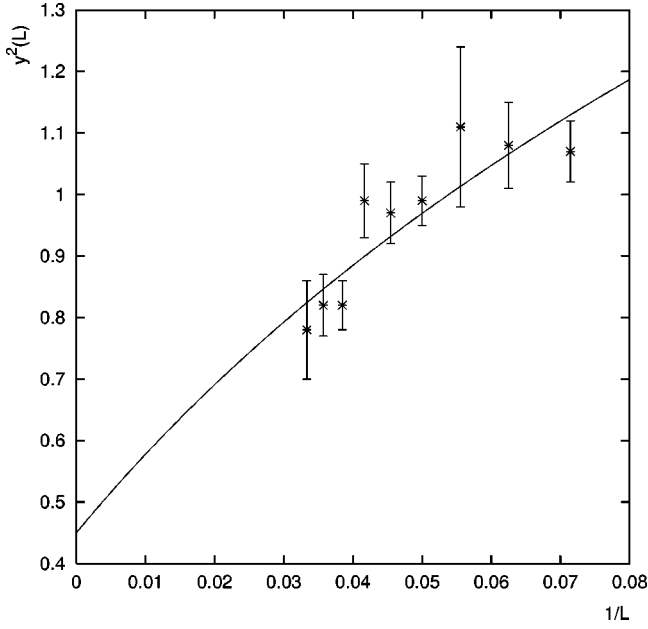
FIG. 7. Fit of the parameter $y^2(L)$ (see Table I) as a function of $1/L$ using $a+\log(1+b/L)$. We obtain $a=0.45(1)$, $b=13.6(45)$, $\chi^2/\text{d.o.f.}=1.05$ and goodness-of-fit $Q=39.3\%$.
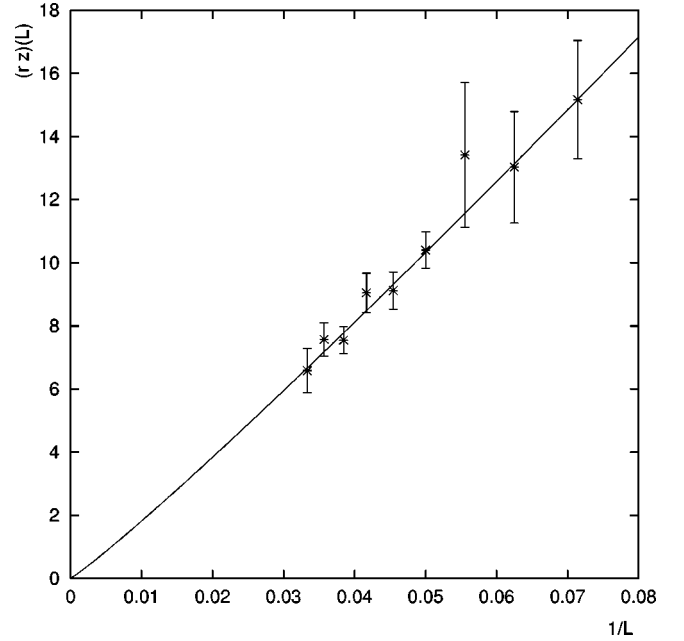

FIG. 8. Fit of the product $(rz)(L)$ (see Table I) as a function of $1/L$ using $\exp(a)/L^b$. We obtain $a=5.6(4)$, $b=1.1(1)$, $\chi^2/\text{d.o.f.}=0.36$ and goodness-of-fit $Q=92.6\%$.

the parameters which we obtain[10] are $\Lambda^2_{\text{coul}}=1.0(2)$, $z=1.2(1)$, $b'=0.18(2)$, $b=0.20(2)$, $\alpha=1.9(3)$, with $\chi^2/\text{d.o.f.}=0.44$ and goodness-of-fit $Q=98.3\%$ using the data for $L=28$ and $L=30$, where $b'\equiv\frac{11}{12}b$. We have checked that similar results are obtained with $\vec{k}^2_{\text{min}}=0.3$ and $\vec{k}^2_{\text{min}}=1.0$ (see Table III) but the resulting $\chi^2/\text{d.o.f.}$ is smallest for $\vec{k}^2_{\text{min}}=0.5$.

The value of $\alpha\sim2$ corresponds to $g^2_{\text{coul}}\sim\text{const}/|\vec{k}|$, and $V(\vec{k})\sim\text{const}/|\vec{k}|^3$ at low momentum. The volume dependence of the data, and therefore of our fit, is quite weak, but one notices in Table III that the value of α decreases as the low momentum cut-off k^2_{min} increases. This corresponds to an increase in the strength of the singularity of $g^2_{\text{coul}}(\vec{k})$ at $\vec{k}=0$ as finite-volume effects are reduced. However, as explained above, we must make an extrapolation in β in order to arrive at any precise conclusion about the strength of the singularity in the continuum limit. Nevertheless, our data at finite β and L clearly indicate a color-Coulomb potential that is more singular than $V(\vec{k})\sim\text{const}/|\vec{k}|^2$ at low $\vec{k}$.

III. CONCLUSIONS

We have used simple formulas to fit the data for the equal-time gluon correlators $D^{\text{tr}}(\vec{k})$ and $D_{44}(\vec{k})$ in $SU(2)$ lattice gauge theory in the minimal lattice Coulomb gauge at $\beta=2.2$. Our fits have the following features:

(i) The equal-time would-be physical gluon propagator

$D^{\text{tr}}(\vec{k},L)$ at *zero* momentum $\vec{k}$ extrapolates to 0 in the limit of infinite lattice volume, i.e. $D^{\text{tr}}(0,\infty)=0$. The rate of approach for lattice volume $V=L^4$ was fit by $D^{\text{tr}}(0,L)=CL^{-b}$, where $b=0.50(1)$. The *vanishing* of the gluon propagator $D^{\text{tr}}(\vec{k})$ at $\vec{k}=0$ is highly counter-intuitive, and the only explanation for it is the suppression of the low momentum components of the gluon field that is a particular feature
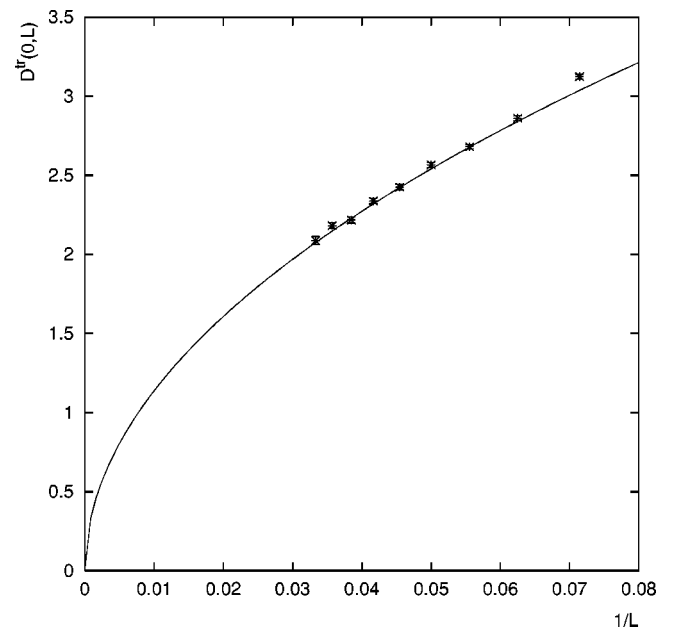

FIG. 9. Fit of the zero-momentum transverse gluon propagator $D^{\text{tr}}(0,L)$ as a function of $1/L$ using $\exp(a)/L^b$. Considering the data for $L\geq16$, we obtain $a=2.43(4)$, $b=0.50(1)$, $\chi^2/\text{d.o.f.}=0.69$ and goodness-of-fit $Q=65.6\%$.
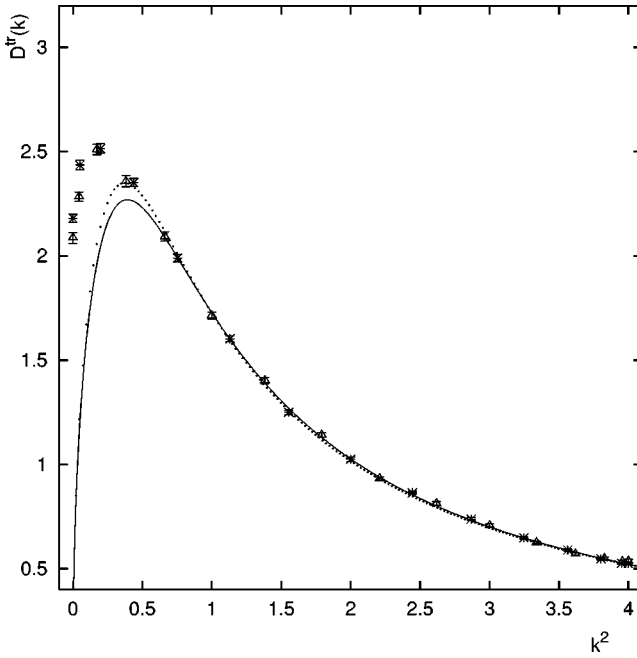
FIG. 10. Plot of the gluon propagator $D^{\mathrm{tr}}(\vec{k})$ as a function of the square of the lattice momentum $\vec{k}^2$ for $L=28$ (*) and 30 ($\triangle$) and fits of these data using Eq. (31) with the parameter values and low momentum cut-offs reported in the fourth (solid line) and fifth (dotted line) rows of Table II. Error bars are one standard deviation.

FIG. 11. Plot of the running coupling constant $\frac{12}{11}g^2_{\mathrm{coul}}(\vec{k})$ $\equiv \vec{k}^2 D_{44}(\vec{k})$ as a function of the square of the lattice momentum $\vec{k}^2$ for $L=28$ (*) and 30 ($\triangle$) and fits of these data using Eq. (34) with the parameter values and low momentum cut-offs reported in the second row of Table III. Error bars are one standard deviation.

of the Gribov horizon, which constitutes the boundary of configuration space.[11]

(ii) Asymptotically at low momentum our fitting formula behaves like $D^{\mathrm{tr}}(\vec{k}) \propto (\vec{k}^2)^\alpha$, with the value extrapolated to infinite lattice volume $\alpha = 0.48(5)$ (see Table II). With the value $x=0$ imposed and a low-momentum cut-off one obtains (from $L=28$ and $L=30$) $\alpha = 0.49(1)$ or $\alpha = 0.51(1)$ (see Table II). This is in striking numerical agreement with Gribov's formula $D^{\mathrm{tr}}(\vec{k}) = (|\vec{k}|/2)[(\vec{k}^2)^2 + M^4]^{-1/2}$, which gives $\alpha = 0.5$.

(iii) We have obtained an excellent 2-pole fit for $D^{\mathrm{tr}}(\vec{k})$. Our fit indicates that the poles occur at *complex* $m^2 = x \pm iy$. The real part x is quite small and compatible with 0. Remarkably, a pole in k^2 at purely imaginary $m^2 = 0 \pm iy$ agrees with the Gribov propagator $D^{\mathrm{tr}}(\vec{k}) = (|\vec{k}|/2)[(\vec{k}^2)^2 + M^4]^{-1/2}$, with $y^2 = M^4$. Note that only a purely imaginary pair of poles gives a correction to the free equal-time propagator $D^{\mathrm{tr}}(\vec{k})$ $\approx |\vec{k}|^{-1}(1 - \frac{1}{2}[M^4/(\vec{k}^2)^2])$ of relative order $(\vec{k}^2)^2$ with coefficient of dimension (mass)^4. It may not be a coincidence that this is the dimension of the gluon condensate $\langle F^2 \rangle$, which is the lowest dimensional condensate in QCD. Because of the gauge invariance of the location of the poles, by

virtue of the Nielsen identities [1], and because of the theoretical suggestiveness of our result, we are encouraged to report the values $m^2 = 0 \pm iy$, for $y = 0.671(7)$ in lattice units, or $y = 0.590(7)$ GeV^2, $M = y^{1/2} = 0.768(4)$ GeV for the location of the gluon poles in k^2.

(iv) The Coulomb gauge offers a definition of the running coupling constant, $\frac{12}{11}g^2_{\mathrm{coul}}(\vec{k}) = \vec{k}^2 D_{44}(\vec{k})$, which has advantages for numerical determination. It is less subject to fluctuation than the determination of g^2 from the 3-point function in the Landau gauge [25], but the extrapolation in β remains to be done.

(v) Our data for $D_{44}(\vec{k})$ require a cut at low momentum to eliminate lattice artifacts. After this cut, the running coupling constant defined by $\frac{12}{11}g^2_{\mathrm{coul}}(\vec{k}/\Lambda_{QCD}) = \vec{k}^2 D_{44}(\vec{k})$ extrapolates to low momentum in accordance with infrared slavery, namely the running coupling constant $g^2_{\mathrm{coul}}(\vec{k}/\Lambda_{QCD})$ diverges in the zero-momentum limit.

(vi) The observed strong *enhancement* of the instantaneous color-Coulomb potential $V(\vec{k})$ and the strong *suppression* of the equal-time would-be physical gluon propagator $D^{\mathrm{tr}}(\vec{k})$ both at low $\vec{k}$, strongly support the confinement scenario of Gribov [6,7]. In addition to this qualitative agreement, we note excellent numerical agreement of our fit to Gribov's formula $D^{\mathrm{tr}}(\vec{k}) = (|\vec{k}|/2)[(\vec{k}^2)^2 + M^4]^{-1/2}$, reported in 1, 2, and 3 above. If this excellent fit is maintained at larger β values, then it appears that we have obtained a quantitative understanding of $D^{\mathrm{tr}}(\vec{k})$.

---

[11]A similar result, i.e. a transverse gluon propagator that at *zero* momentum $\vec{k}$ extrapolates to 0 in the limit of infinite lattice volume V, has been recently obtained for pure $SU(2)$ lattice gauge theory in the three-dimensional case and in the magnetic sector at finite temperature [26].
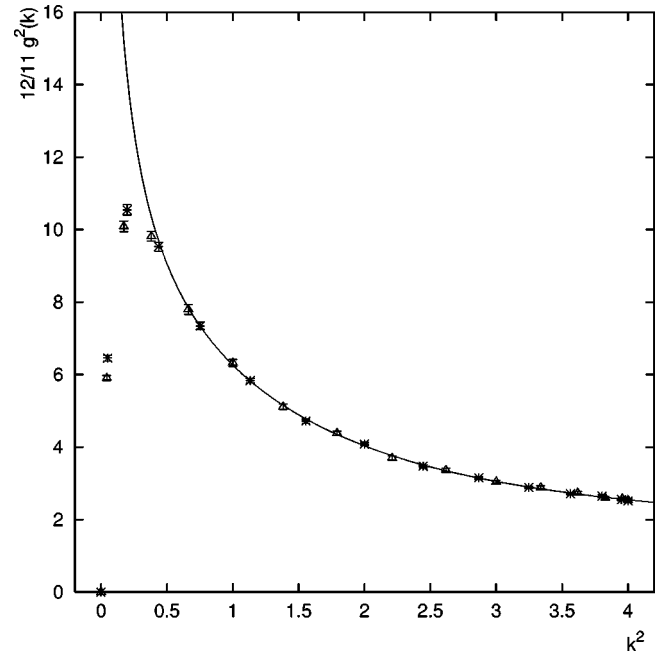
TABLE III. Fit of the running coupling constant $\frac{12}{11}g_{\mathrm{coul}}^2(\vec{k})\equiv\vec{k}^2D_{44}(\vec{k})$ using Eq. (34). The resulting fitting parameters, χ^2/d.o.f. and goodness-of-fit Q are reported for three different values of the low-momentum cut $\vec{k}_{\mathrm{min}}^2$.

$\vec{k}_{\mathrm{min}}^2$	No. data points	$\Lambda_{\mathrm{coul}}^2$	z	$b'=\frac{11}{12}b$	α	χ^2/d.o.f.	Q
0.3	25	0.84(8)	1.14(5)	0.165(9)	2.2(1)	0.59	92.8%
0.5	23	1.0(2)	1.2(1)	0.18(2)	1.9(3)	0.44	98.3%
1.0	20	1.2(9)	1.3(4)	0.19(7)	1.7(7)	0.48	95.8%

ACKNOWLEDGMENTS

APPENDIX: NUMERICAL GAUGE FIXING

The minimal lattice Coulomb gauge is defined by two gauge-fixing steps. In the first step the *spatial* link variables $U_{\vec{x}ti}\in SU(N)$, for $i=1,2,3$, are made as close to unity as possible by minimizing the "horizontal" minimizing function

$$F_{\mathrm{hor},U}(g)\equiv\sum_{\vec{x},t,i}\mathrm{Re}\,\mathrm{Tr}(1-{}^g U_{\vec{x}ti}),\qquad(\mathrm{A}1)$$

with respect to gauge transformations $g_{\vec{x}t}$. The sum extends over all horizontal or space-like links, and the minimization is done independently on each time-slice $t=x_4$. (The gauge transform ${}^g U_{x\mu}$ of the link variable $U_{x\mu}$ is defined by ${}^g U_{xy}\equiv g_x^{-1}U_{xy}g_y$, where $y\equiv x+\hat{\mu}$ and $\hat{\mu}$ is the unit vector in the μ direction.) The stochastic over-relaxation algorithm does not necessarily yield the absolute minimum of the minimizing function but leads in general to one of several local minima. Different minima correspond to different Gribov copies. For the lattice volumes 16^4 and 20^4 we have checked that the dependence of the gluon propagators $D^{\mathrm{tr}}(\vec{k})$ and $D_{44}(\vec{k})$ on which Gribov copy one ends up is of the order of magnitude of the numerical accuracy, in agreement with Ref. [27].

After this step the lattice gluon field is 3-dimensionally transverse [see Eq. (A5) below]. But the gauge fixing is as yet incomplete because it leaves a t-dependent but $\vec{x}$-independent gauge transformation g_t arbitrary. This arbitrariness is fixed in the second step in which the *time-like* link variables $U_{\vec{x}t4}$ are made as close to unity as possible by minimizing the "vertical" minimizing function

$$F_{\mathrm{ver},U}(g)\equiv\sum_{\vec{x},t}\mathrm{Re}\,\mathrm{Tr}(1-{}^g U_{\vec{x}t4}),\qquad(\mathrm{A}2)$$

with respect to $\vec{x}$-independent gauge transformations g_t. The sum extends over all vertical or time-like links. This gauge fixing of the vertical links does not alter the spatial correlator

$D^{\mathrm{tr}}(\vec{k})$ nor the color-Coulomb potential $\mathcal{V}(A^{\mathrm{tr}})$. However it reduces the non-instantaneous part of $D_{44}(\vec{k})$, so that it is suppressed compared to the instantaneous part $V(\vec{k})$ and vanishes with the lattice spacing in the continuum limit.

This gauge fixing, in which first F_{hor} is minimized and then F_{ver} is minimized is equivalent to the limit of the interpolating gauge in which the single function, depending on a real positive parameter λ,

$$F=F_{\mathrm{hor}}+\lambda F_{\mathrm{ver}}\qquad(\mathrm{A}3)$$

is minimized, and the limit $\lambda\to 0$ is taken.

With this gauge fixing, the link variables should approach unity in the continuum limit in the sense that $\lim_{\beta\to\infty}(1/2)\mathrm{Tr}(U_{x\mu})=1$. In our study at $\beta=2.2$ we obtain $\langle(1/2)\mathrm{Tr}(U_{xi})\rangle=0.86249(3)$ for the space-like links, whereas for time-like links $\langle(1/2)\mathrm{Tr}(U_{x4})\rangle=0.221(6)$ on lattice volume 14^4. (The dependence on the volume is not strong.) Thus we are quite far from the continuum limit for quantities such as $V(\vec{k})$ that depend on the vertical links, and they may exhibit significant β-dependence in the extrapolation to the continuum limit. This will be reported subsequently.

The gauge fixing just described produces a configuration U which is a local minimum of $F_{\mathrm{hor},U}(g)$ and $F_{\mathrm{ver},U}(g)$ at $g=1$. At a local minimum the minimizing functions are (i) stationary under infinitesimal variations $\delta F=0$ and (ii) the matrix of second variations of the minimizing function is non-negative, $\delta^2 F\geq 0$. We now comment on implications of these properties for gauge-fixed configurations U. At a local minimum, the horizontal minimizing function $F_{\mathrm{hor},U}(g)$ is stationary with respect to infinitesimal variations $g_x\to g_x(1+\omega_x)$. Here $\omega_x=t^a\omega_x^a$ is an element of the Lie algebra of the $SU(N)$ group, with anti-Hermitian basis t^a satisfying $[t^a,t^b]=f^{abc}t^c$ and $\mathrm{Tr}(t^a t^b)=-\frac{1}{2}\delta^{ab}$. The corresponding variation of F_{hor} is given by

$$\delta F_{\mathrm{hor},U}(g)=-\frac{1}{2}\sum_{\vec{x},i}\mathrm{Tr}[(\omega_{\vec{x}+\hat{i},t}-\omega_{\vec{x}t})({}^g U_{\vec{x}ti}-{}^g U_{\vec{x}ti}^{\dagger})].$$
$$(\mathrm{A}4)$$

For a configuration U which is a local minimum (at $g_x=1$), this quantity must vanish for all $\omega_{\vec{x}t}$, which gives

$$\sum_i(A_{\vec{x},t,i}-A_{\vec{x}-\hat{i},t,i})=0.\qquad(\mathrm{A}5)$$

Here $A_{\vec{x},t,i}$ is the lattice gluon field defined by

$$A^a_{x\mu} \equiv -\text{Tr}[t^a(U_{x\mu} - U^\dagger_{x\mu})], \qquad (A6)$$

which is a lattice analog of the continuum connection $A^a_\mu(x)$. Equation (A5) is the lattice transversality condition for spatial directions, which is the defining condition for the lattice Coulomb gauge.

Since the gauge-fixed configuration U is a local minimum of $F_{\text{hor},U}(g)$ (at $g_x = 1$), its second variation is non-negative

$$\delta^2 F_{\text{hor},U}(g) = (\omega, M(U)\omega) \geq 0 \quad \text{for all} \quad \omega. \qquad (A7)$$

Here $M(U)$ is the lattice Faddeev-Popov matrix defined on a given time-slice t by

$$(\omega, M(U)\omega) \equiv -\frac{1}{2} \sum_{x,i} \text{Tr}[(\omega_{x+\hat{i}} - \omega_x)(U_{xi}\omega_{x+\hat{i}} - \omega_x U_{xi} \\ + \omega_{x+\hat{i}}U^\dagger_{xi} - U^\dagger_{xi}\omega_x)], \qquad (A8)$$

and we have suppressed the index t which is common to all variables. The positivity of $M(U)$ is a condition on configu-

rations U which, together with the transversality condition (A5), defines the lattice Gribov region, whose boundary is the Gribov horizon.

[That this is a highly restrictive condition is suggested by the following consideration. The Faddeev-Popov matrix $M(U)$ for $SU(N)$ gauge theory is a symmetric matrix of dimension $V(N^2-1)$, where V is the (large) number of sites of the lattice, so it has $V(N^2-1)$ eigenvalues. Configuration space is divided into $V(N^2-1)+1$ different regions R_n according to the number $n = 0, \ldots, V(N^2-1)$ of positive eigenvalues of $M(U)$. Of these, the Gribov region consists of the single region $R_{V(N^2-1)}$ that includes $U_{xi} = 1$. For the $SU(2)$ group at least, all regions are populated. To see this, observe that for $U_{x\mu} = 1$, we have $M(1) = -\Delta$, whereas for $U_{x\mu} = -1$, we have $M(-1) = \Delta$, where Δ is the lattice Laplacian. In these 2 cases, depending on the sign, the configuration $U = \pm 1$ is in region $R_{V(N^2-1)}$ or R_0. By continuity therefore all $V(N^2-1)+1$ different regions are populated. Similar considerations apply to $F_{\text{ver},U}(g)$.]

[1] N.K. Nielsen, Nucl. Phys. **B101**, 173 (1975).
[2] R.E. Cutkosky, Phys. Rev. D **30**, 447 (1984).
[3] C. Parrinello, S. Petrarca, and A. Vladikas, Phys. Lett. B **268**, 236 (1991).
[4] K.M. Decker and Ph. de Forcrand, Nucl. Phys. B (Proc. Suppl.) **17**, 567 (1990).
[5] A. Cucchieri and T. Mendes, Nucl. Phys. **B471**, 263 (1996).
[6] V.N. Gribov, Nucl. Phys. **B139**, 1 (1978).
[7] D. Zwanziger, Nucl. Phys. **B518**, 237 (1998).
[8] N.H. Christ and T.D. Lee, Phys. Rev. D **22**, 939 (1980).
[9] D. Zwanziger, Nucl. Phys. **B485**, 185 (1997).
[10] D. Zwanziger, Nucl. Phys. **B378**, 525 (1992).
[11] D. Zwanziger, Nucl. Phys. **B364**, 127 (1991).
[12] A. Cucchieri and D. Zwanziger, following article, Phys. Rev. D **65**, 014002 (2002).
[13] A. Cucchieri and D. Zwanziger, Phys. Rev. Lett. **78**, 3814 (1997).
[14] A. Szczepaniak et al., Phys. Rev. Lett. **76**, 2011 (1996).
[15] D.G. Robertson et al., Phys. Rev. D **59**, 074019 (1999).
[16] L. Baulieu and D. Zwanziger, Nucl. Phys. **B581**, 604 (2000).
[17] L. Baulieu, P.A. Grassi, and D. Zwanziger, Nucl. Phys. **B597**, 583 (2001).
[18] A. Cucchieri, Nucl. Phys. **B521**, 365 (1998).
[19] L. Baulieu and D. Zwanziger, Nucl. Phys. **B548**, 527 (1999).
[20] D. Becirevic et al., Phys. Rev. D **61**, 114508 (2000).
[21] J. Fingberg, U. Heller, and F. Karsch, Nucl. Phys. **B392**, 493 (1993).
[22] C. Bernard, C. Parrinello, and A. Soni, Phys. Rev. D **49**, 1585 (1994).
[23] D.B. Leinweber et al., Phys. Rev. D **60**, 094507 (1999); **61**, 079901 (2000).
[24] A. Cucchieri and T. Mendes, in *Strong and Electroweak Matter '98*, edited by J.Ambjørn et al. (World Scientific, Singapore, 1999); A. Cucchieri, *The Lattice Gluon Propagator into the Next Millennium*, in *Understanding Deconfinement in QCD*, edited by D. Blaschke, F. Karsch, and C. D. Roberts (World Scientific, Singapore, 2000).
[25] B. Alles et al., Nucl. Phys. **B502**, 325 (1997); P. Boucaud et al., J. High Energy Phys. **10**, 017 (1998).
[26] A. Cucchieri, F. Karsch, and P. Petreczky, Phys. Lett. B **497**, 80 (2001).
[27] A. Cucchieri, Nucl. Phys. **B508**, 353 (1997).